Classical spin model of the relaxation dynamics of rare-earth doped permalloy

ELLIS, M. O. A., OSTLER, Thomas <http://orcid.org/0000-0002-1328-1839> and CHANTRELL, R. W.

Classical spin model of the relaxation dynamics of rare-earth doped permalloy

M. O. A. Ellis,* T. A. Ostler, and R. W. Chantrell
Department of Physics, University of York, York, YO10 5DD, United Kingdom
(Received 4 April 2012; revised manuscript received 24 September 2012; published 19 November 2012)

In this paper, the ultrafast dynamic behavior of rare-earth doped permalloy is investigated using an atomistic spin model with Langevin dynamics. In line with experimental work, the effective Gilbert damping is calculated from transverse relaxation simulations, which shows that rare-earth doping causes an increase in the damping. Analytic theory suggests that this increase in damping would lead to a decrease in the demagnetization time. However, longitudinal relaxation calculations show an increase with doping concentration instead. The simulations are in a good agreement with previous experimental work of Radu *et al.* [Radu *et al.*, Phys. Rev. Lett. **102**, 117201 (2009)]. The longitudinal relaxation time of the magnetization is shown to be driven by the interaction between the transition metal and the laser-excited conduction electrons, whereas the effective damping is predominantly determined by the slower interaction between the rare-earth elements and the phonon heat bath. We conclude that for complex materials, it is evidently important not to expect a single damping parameter but to consider the energy transfer channel relevant to the technique and time scale of the measurement.

DOI: 10.1103/PhysRevB.86.174418 PACS number(s): 75.78.Jp, 75.50.Gg, 75.10.Hk

I. INTRODUCTION

Over the last decade ultrafast magnetization dynamics has proved to be a complex and expanding field of magnetism research. The increasing use of femtosecond lasers[1–3] to probe magnetic properties on the time scale of the exchange interaction have been driven by the need to understand and control the behavior of magnetic materials. Such control is potentially important for future applications. The research was initiated by the pioneering work of Beaurepaire *et al.*[4] who first observed the subpicosecond collapse of magnetic order in ferromagnetic nickel using femtosecond laser pulses. The results showed that after a laser pulse, the magnetization responds within the first picosecond leading to a sharp demagnetization and a much longer remagnetization time. These dynamics have been observed by other experimental groups[5,6] but the theoretical understanding of the dynamics is still limited. Improving this understanding could pave the way for magnetic storage devices with operating speeds much faster than those of present devices.

Recently, there has emerged a strong interest in the properties of GdFeCo following the discovery[2] that circularly polarized laser light gives rise to magnetization reversal in the absence of an externally applied field. In this work, we concentrate on the use of linearly polarized light for which the heating caused by the laser pulse drives the dynamic behavior. The focus of the current paper is on the understanding of energy transfer channels in rare-earth (RE)/transition metal (TM) alloys, which ultimately is necessary for a complete understanding of optomagnetic reversal and of the phenomenon of heat-driven magnetization reversal.[7]

Specifically, we focus on the relationship between the magnetization dynamics, as characterized by the demagnetization time following a laser pulse, and the intrinsic damping of the material. Recent theoretical work by Koopmans *et al.*[8] used a model based on Elliot-Yafet scattering of electrons on impurities and phonons. An approximate relationship for the characteristic demagnetization time is derived:

$$\tau_d \approx \frac{c_0 \hbar}{k_B T_C \alpha}, \tag{1}$$

where c_0 is a material based parameter, T_C is the Curie temperature, and α is the Gilbert damping factor.[9] This theoretical model gives an inverse relationship between the Gilbert damping and the demagnetization time, implying that for larger damping the magnetization will demagnetize faster. Koopmans' work shows that this equation gives values that are of the correct order of magnitude for certain results, such as nickel, but it does not provide quantitative predictions.

Kazantseva *et al.*[10] derive a similar result based on the assumption that the thermal noise from the Langevin dynamics is the dominant process in the demagnetization giving

$$\tau_d \approx \frac{\mu_s}{2\lambda\gamma k_B T_e}, \tag{2}$$

where γ is the gyromagnetic ratio, T_e is the electron temperature, and μ_s is the magnitude of the atomic magnetic moment. Equation (2) matches Koopmans' model well and also predicts a dependence of τ_d on the spin magnitude μ_s. This is borne out by the experiments and calculations[1] showing differential relaxation of the magnetization of the RE and TM sublattices in GdFeCo.

λ is the atomistic level coupling parameter arising in the Langevin equation of the system. λ is analogous to α on the atomistic scale, as they describe the direct transfer of angular momentum into and out of the system. This parameter encompasses an array of physical processes that mediate the energy transfer. It is therefore crucial for the fundamental understanding of magnetization dynamics and the possibility of designing new magnetic devices.

The damping is a measurable quantity, determined, for example, via ferromagnetic resonance (FMR) studies,[11] but as shown by Chubykalo-Fesenko *et al.*,[12] it is important to distinguish between the macroscopic and the microscopic parameters. Importantly, the macroscopic damping contains nonlinear effects that transfer energy which are not due to the direct damping, such as the excitation of spin waves, which removes energy from the FMR ($k = 0$) mode. Reference 12 shows, using an atomistic model, that the macroscopic α is temperature dependent even though the atomic level parameter λ remains constant; the values of λ and α only coinciding at

$T = 0$ K. We therefore distinguish between the macroscopic effective Gilbert damping parameter α_{eff}, which is calculable from FMR measurements and the direct Gilbert damping α, that is present in Eqs. (1) and (2). These values must be interpreted, in the spirit of the original derivations, as the damping values at the atomic level.

The predicted relationship between τ_d and α was investigated experimentally by Radu *et al.*[13] The study aimed to use the known dependence of the damping constant of permalloy ($Ni_{80}Fe_{20}$) on the addition of RE impurities[14] to investigate how this changed the demagnetization time. A series of RE doped permalloy samples of different concentrations were prepared and FMR measurements showed the expected increase of damping constant with RE concentration. However, the predicted decrease of τ_d with α was not observed in subsequent demagnetization measurements using ultrafast laser pulses. In fact, a slight increase of τ_d with RE concentration was found, in contradiction to the theoretical predictions.

Other theoretical work of Fähnle *et al.*[15] also predicts a relation between the damping and the demagnetization time using "effective field theories." This takes into account the electronic structure in greater detail and arrives at two different relations depending on the dominant component of the damping. The "conductivity-like" contributions to the damping lead to the "breathing Fermi-surface" model, which predicts a linear relation between the damping and demagnetization time. The other "resistivity-like" damping contributions give a "bubbling Fermi-surface" model, which then predicts an inverse relation instead. This supports both of the different results of Refs. 8 and 13 under different regimes.

In the present study, we investigate the effect of RE doping on the dynamic properties of permalloy using atomistic spin dynamics (ASD).[16] Using this method, the nonequilibrium dynamics at a finite temperature can be described using the Landau-Lifshitz-Gilbert Langevin equation.[17] To quantify the demagnetization time from the simulations, the integral relaxation time[18] (IRT) is used.

The model incorporates two thermal reservoirs; representing the conduction electrons and the lattice, the thermodynamics of which are represented by the two-temperature model.[19,20] The heating of the laser pulse acts directly on the electron reservoir which then transfers the energy into the lattice reservoir via electron-phonon interactions. Within the ASD model, the mechanism that drives the demagnetization of the material is the elevated temperatures causing random orientation of the magnetic moments, rather than the reduction in the magnitude of the moments. These two thermal reservoirs are coupled to the spin dynamics using two separate coupling parameters.[21]

This paper is organized as follows. First, the atomistic spin dynamics model is introduced along with the extended Heisenberg spin Hamiltonian and the Landau-Lifshitz-Gilbert Langevin equation. A description of the two-temperature model and the use of Langevin dynamics to model the thermal noise follows, leading to a description of the the dynamic simulations that were performed. The results of the simulations are in a good agreement with the experiments of Radu *et al.*[13] We conclude that in complex materials it is important not to expect a single damping parameter but to consider the energy transfer channel relevant to the technique and time scale of the measurement.

II. DESCRIPTION OF THE MODEL

The model used is a classical spin model described in detail in Refs. 16 and 22 and is outlined briefly here. The system is viewed on an atomistic scale with each atom having an associated magnetic moment. The basis of the model is the numerical solution of a set of coupled Landau-Lifshitz-Gilbert (LLG) equations of motion for the magnetic moments in an effective field. The effective field combines the Hamiltonian contribution and a thermal noise contribution. Each magnetic moment is normalized, such that $\mathbf{S} = \boldsymbol{\mu}/|\mu_s|$, where μ_s is the magnitude of the magnetic moment, hereafter noted as μ_i to represent the magnitude at site i. The spin moments are of constant magnitude and there is no fluctuations in the magnitude of the localized magnetic moment.

An extended Heisenberg spin Hamiltonian is used, comprised of exchange, uniaxial anisotropy, and Zeeman energies. The Hamiltonian is given by

$$\mathcal{H} = -\sum_{i \neq j} J_{ij}\, \mathbf{S}_i \cdot \mathbf{S}_j - \sum_i d_z\, \mathbf{S}_{i,z}^2 - \sum_i \mu_i\, \mathbf{S}_i \cdot \mathbf{B}. \quad (3)$$

Here, J_{ij} is the exchange integral between spins i and j, limited here to nearest neighbors, d_z is the uniaxial anisotropy constant along the z axis, $\mathbf{S}_i$ is the normalized spin at site i, and $\mathbf{B}$ is the applied field in tesla.

The system acts as a dilute ferrimagnet with two separate ferromagnetic sublattices; the permalloy (TM) sublattice is dominant with only small concentrations of RE doping and most of the behavior evolves from this. The exchange interaction between the TM and RE is antiferromagnetic, giving rise to an antiparallel ground state below the Curie temperature. We assume that the RE spins have ferromagnetic exchange between themselves, but weaker than that of the TM exchange.

The magnetization dynamics is described by the Landau-Lifshitz-Gilbert equation.[23] For atomic spins, it is written as

$$\frac{\partial \mathbf{S}_i}{\partial t} = -\frac{\gamma_i}{\left(1+\lambda_i^2\right)\mu_i}\mathbf{S}_i \times (\mathbf{H}_{\text{eff}} + \lambda_i\, \mathbf{S}_i \times \mathbf{H}_{\text{eff}}). \quad (4)$$

It is important to point out that the parameters γ_i, λ_i, and μ_i are site dependent and vary depending on the species,[22] but here to restrict the set of open parameters, we assume γ_i is constant.

To couple the thermal reservoirs into the spin system, Langevin dynamics[17] is applied using a stochastic noise term. This converts the LLG equation into a stochastic differential equation, which can be written as a standard Langevin equation with multiplicative noise. The effective field, $\boldsymbol{H}_{\text{eff}}$, is derived from the Hamiltonian and a thermal noise term $\boldsymbol{\zeta}$:

$$\mathbf{H}_{\text{eff}} = -\frac{\partial \mathcal{H}}{\partial \mathbf{S}} + \boldsymbol{\zeta}. \quad (5)$$

The thermal noise term is a stochastic process, that is, parameterized by using the Fokker-Planck equation. Since the coupling parameter controls the energy flow out of the system,

it is found that it also controls the strength of the stochastic process and thus the energy flow into the system.

The stochastic process requires a well-defined temperature, which scales the strength of the noise. To that end, we employ the two-temperature model.[10,20] The two-temperature model defines an temperature associated with that of the conduction electrons and the phonons after laser excitation. The two act as reservoirs to which the spin system can be coupled. The time dependence of the heating (assumed uniform across the sample) can be represented by two coupled differential equations:

$$C_e \frac{dT_e}{dt} = -G_{\rm el}(T_l - T_e) + P(t), \tag{6}$$

$$C_l \frac{dT_l}{dt} = -G_{\rm el}(T_e - T_l). \tag{7}$$

In the simulations, the electron-phonon coupling factor $G_{\rm el}$ and the lattice specific heat capacity C_l are taken to be independent of temperature, which for the room temperature calculations is a reasonable assumption. Lin *et al.*[24] show that the electron-coupling factor is reduced by the excitation of d-band electrons but this occurs at high temperatures and so this effect should be minimal in the situations considered here. The parameters used were $G_{\rm el} = 1.7 \times 10^{18}\,{\rm J\,m^{-3}\,K^{-1}\,s^{-1}}$, $C_l = 3 \times 10^6\,{\rm J\,m^{-3}\,K^{-1}}$ and $C_e(T_e) = 7 \times 10^2\,T_e\,{\rm J\,m^{-3}\,K^{-1}}$. Using these parameters, the relevant time scale of the lattice temperature dynamics can be calculated; the electron-phonon coupling time, which is $C_l/G_{\rm el} = 1.765$ ps, that describes the exponential decay of the lattice temperature towards a constant electron temperature.

We couple the TM species to the electron system, this is based on previous studies of fast relaxation in transition metals,[10] which concluded that only a coupling of the TM to the conduction electrons was sufficient to cause subpicosecond demagnetization. This is consistent for metals with the mechanism of Fähnle *et al.*[15]

The energy transfer mechanisms in the RE species are more complex. The $4f$ electrons exhibit a strong spin-orbit coupling, with spherical orbitals for Gd and nonspherical for Ho. This leads to a large anisotropy in Ho and also a large damping. Rebei and Hohlfeld[25] have studied damping in the RE metals arising from spin/lattice interactions and show that the damping is relatively large in the Lanthanide series, but is low for Gd. As discussed by Wietstruk *et al.*,[26] the nonspherical orbits, in their case for Tb, provide a coupling between the magnetic moments with the motion of the lattice, while the spherical orbits of Gd do not provide this mechanism. Thus here we assume that the transfer of energy and momentum is via spin/lattice interactions for Ho and via spin/conduction electrons for Gd. This opens the possible coupling channels between the two-temperature model and the RE spin system; therefore two coupling parameters $\lambda_e^{\rm RE}$ and $\lambda_l^{\rm RE}$ are defined.[21]

For Gd, it is shown by Seib *et al.*[27] that there is an effective damping arising from a coupling of the localized $4f$ electrons direct damping and the indirect damping of $5d6sp$ conduction electrons. In Ref. 27, the contribution of the $5d6sp$ electrons is in itself large but the effective contribution is weak and comparable to the damping in Co. The direct $4f$ contribution is, however, not known and thus which contribution dominates the effective damping is unknown.

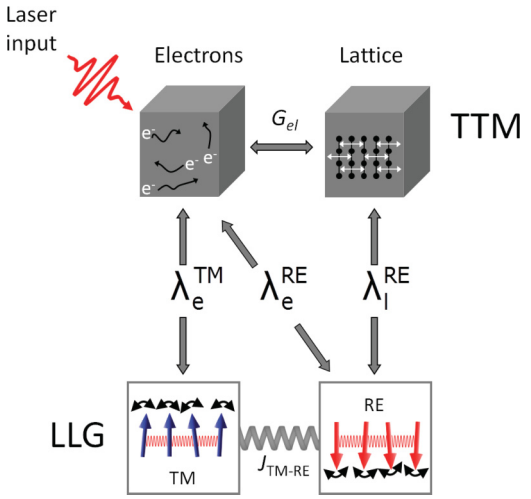

FIG. 1. (Color online) A schematic representing energy transfer channels between the thermal reservoirs of the two-temperature model (TTM) and the spin system, the dynamics of which is described by the Landau-Lifshitz-Gilbert (LLG) equation. The Gaussian profile represents the effect of laser heating, which is coupled to the electron temperature. The electron reservoir is coupled to the lattice reservoir via the coupling constant $G_{\rm el}$. The transition metal (TM) spins, which in our case are Ni and Fe, are then coupled to the electron temperature. The rare-earth (RE) element, Ho or Gd, is coupled to either the electron or lattice temperature. The TM and RE spins are coupled via antiferromagnetic exchange giving rise to an antiparallel ground state.

Figure 1 shows a schematic of the various energy transfer channels between the thermal reservoirs of the two temperature model (TTM) and the spin system. This serves to define the coupling constants used in the model.

The stochastic process is assumed to be white noise with the following mean and variance:

$$\langle \zeta_{i,a}(t) \rangle = 0, \tag{8}$$

$$\langle \zeta_{i,a}(t)\zeta_{j,b}(t') \rangle = \delta_{ij}\delta_{ab}\delta(t - t')D_{\rm llg}, \tag{9}$$

where a and b refer to the components of the spin vector and i and j to separate spins. $D_{\rm llg}$ is the strength of the stochastic process and for the different species, we define the separate coupling channels:

$$D_{\rm llg} = \begin{cases} \frac{2\mu_i k_{\rm B}}{\gamma_i}\lambda_e^{\rm TM} T_e, & \text{TM spins,} \\ \frac{2\mu_i k_{\rm B}}{\gamma_i}\left(\lambda_e^{\rm RE} T_e + \lambda_l^{\rm RE} T_l\right), & \text{RE spins.} \end{cases} \tag{10}$$

The RE coupling factors for the separate baths form the total RE coupling in the LLG equation with a total damping $\lambda_i^{\rm RE} = \lambda_e^{\rm RE} + \lambda_l^{\rm RE}$. T_e and T_l are the temperatures of the electron and lattice bath, respectively, as described by the two-temperature model. We note that the model is based on energy transfer and does not explicitly conserve energy or angular momentum.

The numerical scheme used in the simulations is the semi-implicit scheme defined by Ref. 28, which is a symplectic integrator that conserves the magnitude of the spin length, a requirement of the model. The basis of the scheme is the implicit midpoint scheme as given in Ref. 29. However, to

reduce the computational effort, an approximation is made in predictor-corrector style:

$$\mathbf{S}'_n = \mathbf{S}_n - \frac{\mathbf{S}_n + \mathbf{S}'_n}{2} \times \mathbf{A}(\mathbf{S}_n), \tag{11}$$

$$\mathbf{S}_{n+1} = \mathbf{S}_n - \frac{\mathbf{S}_n + \mathbf{S}_{n+1}}{2} \times \mathbf{A}\left(\frac{\mathbf{S}_n + \mathbf{S}'_n}{2}\right), \tag{12}$$

$$\mathbf{A}(\mathbf{S}) = \frac{\gamma \Delta t}{(1+\lambda^2)\mu}[\mathbf{H}_{\text{eff}}(\mathbf{S}) + \lambda\, \mathbf{S} \times \mathbf{H}_{\text{eff}}(\mathbf{S})]. \tag{13}$$

If we just consider a single step and express the cross product as a matrix, skew $[\mathbf{v}] \cdot \mathbf{w} = \mathbf{v} \times \mathbf{w}$, then the equations for a single site can be solved to give an explicit form:

$$\mathbf{S}_{n+1} = \mathbf{S}_n + \tfrac{1}{2}\text{skew}\,[\mathbf{A}]\mathbf{S}_{n+1} + \tfrac{1}{2}\text{skew}\,[\mathbf{A}]\mathbf{S}_n = \text{Cay}(\mathbf{A})\mathbf{S}_n, \tag{14}$$

where Cay($\mathbf{A}$) is known as the Cayley transform which has the solution given by[30]

$$\text{Cay}(\mathbf{A})\mathbf{X} = \mathbf{X} + \frac{\mathbf{A} \times \mathbf{X} + \frac{1}{2}\mathbf{A} \times \mathbf{A} \times \mathbf{X}}{1 + \frac{1}{4}|A|^2}. \tag{15}$$

The importance of using the Cayley transform is that it applies a rotation to the spin vector rather than a translation thus conserving the spin length. The crucial choice is the input to $\mathbf{A}$; one can choose a single step similar to an Euler method or in this case, our semi-implicit scheme uses a predictor-corrector step and so is equivalent to a Cayley version of the Heun scheme shown in Ref. 30. In general, due to the orthogonal nature of the Cayley transform, an addition of a parallel term, $\mathbf{A}' = \mathbf{A} + \sigma\mathbf{S}$, can be utilized to optimize the scheme.[30,31] However, this only has the effect of overdamping the system, which does not allow the important dynamics to be observed. As with all numerical schemes, the semi-implicit scheme does have an error associated with the approximation. Specifically, while having good convergence for equilibrium properties, it has a larger error in the precession frequency when the exchange field is included. This error decreases for smaller time steps and as such $\Delta t = 1 \times 10^{-16}$s was found to be suitably small enough.

III. RESULTS

Our aim is to compare our spin model results with the measurements of Radu *et al.* in Ref. 13 in order to obtain insight into the energy transfer processes in ferrimagnets. We require studies of longitudinal and transverse relaxation to calculate the demagnetization time and the effective Gilbert damping respectively. Afterwards, we make a direct comparison to the theory and experiment. The computational results are in excellent qualitative agreement with experiment, giving important insight into energy channels and damping mechanisms in ferrimagnets.

Usually permalloy thin films are polycrystalline with a face centered cubic (fcc) structure. Since the RE concentrations in Ref. 13 are low, we assume a fixed lattice for the atomistic model. The polycrystalline structure is simplified to be a single fcc crystal with periodic boundary conditions. For the magnetic moments, we use the values:[32] $\mu_{\text{Ni}} = 0.98\,\mu_B$, $\mu_{\text{Fe}} = 2.31\,\mu_B$, $\mu_{\text{Ho}} = 10.6\,\mu_B$, and $\mu_{\text{Gd}} = 7.94\,\mu_B$. The exchange coupling between the spins is ferromagnetic for TM-TM and RE-RE interactions and antiferromagnetic for the TM-RE interaction using the values $J_{\text{TM-TM}} = 3.60 \times 10^{-21}J$, $J_{\text{RE-RE}} = 1.26 \times 10^{-21}J$, and $J_{\text{TM-RE}} = -1.09 \times 10^{-21}J$. These exchange parameters are derived from standard relations between the exchange and the Curie temperature.

As discussed in the last section, the coupling factors for the TM and Gd are relatively small, while the coupling of Ho is rather high. These quantities are not the Gilbert damping parameters and on a atomistic scale are not well known. The values are taken within the ranges shown in Rebei *et al.*[25] and as such we take the TM and Gd coupling to be $\lambda_e^{\text{TM}} = \lambda_e^{\text{Gd}} = 0.05$ and the Ho coupling to be $\lambda_l^{\text{Ho}} = 0.5$.

To calculate the longitudinal relaxation time of each species, we begin with our system in the antiparallel ground state at 0 K. We then apply a Heaviside step function to 300 K to the electron temperature to represent the inital part of a square heat pulse. Since the system needs only be simulated until it reaches equilibrium, a reasonable time scale is 50 ps, which allows a large system size, 18 nm^3.

The demagnetization time from an ordered to a more disordered magnetic state is characterised by exponential decay, described by a weighted sum with different time constants. In Ref. 13, the demagnetization only occurs for about 200 fs and as a result a single exponential fit is satisfactory. However, during these simulations, the demagnetization is observed over a longer scale and as such, fitting to multiple exponentials does not fit well. Consequently, the integral relaxation time[18] is a much better quantification of the demagnetization time as this already accounts for all of the eigenmodes. The integral relaxation time is calculated using

$$\tau_{\text{IRT}} = \int_0^\infty \frac{\langle M_z(t)\rangle - \langle M_z(\infty)\rangle}{\langle M_z(0)\rangle - \langle M_z(\infty)\rangle}\, dt. \tag{16}$$

Here, M_z is the z component of the magnetization vector where z is our anisotropy axis and the magnetization vector is initially oriented along this axis. Since both the TM and RE sublattices relax differently, the IRT is calculated separately for either sublattice.

It was mentioned earlier that the effective damping as observed in the experiments is not necessarily equivalent to the atomic scale damping which must be used in the spirit of the derivation of Eqs. (1) and (2). However, we proceed along the lines of the experiments to effect a direct comparison with the measurements and to allow interpretation of the underlying physics.

The effective Gilbert damping of our RE doped permalloy system is calculated from the transverse relaxation of the total magnetization. These simulations are independent of the laser induced dynamics and instead show the Gilbert damping through FMR-like methods. This is done by equilibrating the system with an applied field, $h = 0.25$ T, along the anisotropy axis at a constant temperature of 1 K. We then perform a coherent rotation of all of the spins to an angle of 30 degrees in the yz plane. The system then undergoes a relaxation back to equilibrium. The x component of the magnetization is then fitted to using the function $M_x(t) = A\,\cos(t/\tau_p)/\cosh(t/\tau_r + d)$. Within this equation τ_p and τ_r are the precession and transverse relaxation times, respectively. They have the form $\tau_p = (1+\alpha_{\text{eff}}^2)/\gamma h$, $\tau_r = \tau_p/\alpha_{\text{eff}}$. A and d are parameters used to match the equilibrated length of the

magnetization and the initial phase of spin. The damping can be found using the relation between the precession and transverse relaxation times; $\alpha_{\text{eff}} = \tau_p/\tau_r$. The results of the calculation of the effective damping parameter are found to be consistent with experimental observations.[13,33]

A. Longitudinal relaxation calculations

We have performed calculations of the longitudinal relaxation time demonstrating the differential response of the TM and RE sublattices, which is consistent with the results of Ref. 1. In general, the magnetization relaxes as an exponential decay, starting at some initial value at $t = 0$ and decaying to a new equilibrium value.

In TM-RE materials, since the sublattices are oppositely aligned, the demagnetization of the sublattices can actually cause the total magnetization to rise depending on which sublattice is dominant. Due to this behavior, it is useful to characterize the demagnetization time of each sublattice separately rather than the total magnetization. In the experiments of Ref. 13, the magneto-optic Kerr effect is used to measure the magnetization dynamics and consequently, since the TM sublattice provides the dominant signal, the calculated demagnetization time will be linked to this sublattice.

Figure 2(a) shows the relaxation of a 8% doped permalloy system to the temperature profile in Fig. 2(b). It is clear from Fig. 2(a) that the TM sublattice (solid blue line) relaxes much faster than that of the Ho sublattice (red dashed line). This is due to the fact that the TM spins are coupled to the electron temperature and also have a lower moment giving rise to a shorter longitudinal relaxation time according to Eq. (2). The Ho spins take longer to relax due to their coupling to the phonon bath and their larger magnetic moment.[1] The total magnetization (dot-dashed black line) relaxes in a rather complex manner as the two sublattices have completely different time scales.

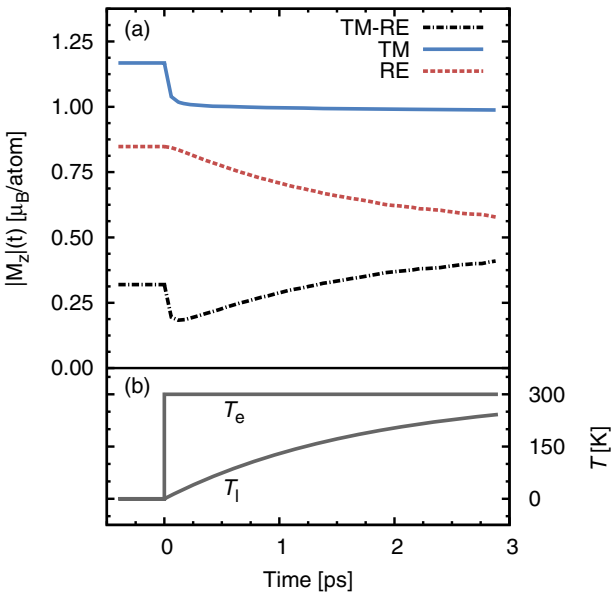

FIG. 2. (Color online) (a) The z component of the total (dot-dashed black line), TM (solid blue line), and RE (red dashed line) magnetization as a function of time for $Ni_{72}Fe_{20}Ho_8$ after a change in temperature from 0 to 300 K. The TM spins are coupled to the electron temperature, while the RE spins are coupled to the phonon temperature. The TM spins respond faster to the increase in temperature while the RE spins takes much longer, these different time scales cause the total magnetization to first demagnetize following the TM behavior before the demagnetization of the RE occurs. The behavior of the electron and phonon temperatures, after a step change in the electron temperature, are shown in (b). By comparing the lattice temperatures dynamics to the RE, we can see the RE spins demagnetize at a similar rate.

Since the TM sublattice has almost completely relaxed within 200 fs, during which time the RE sublattice has only relaxed by a few percent of saturation, the total magnetization initially decreases following the TM magnetization. However, on longer time scales for which the TM lattice is almost in equilibrium, the RE sublattice slowly relaxes. Since the sublattices are oppositely aligned, this slow reduction in the RE lattice manifests as an increase in the total magnetization.

It is worth noting that the relaxation time of the TM sublattice is comparable to the experimentally measured values of τ_d, with the RE relaxing on a significantly longer time scale. This is consistent with the time-resolved magneto-optic Kerr effect signal originating in the TM signal rather than the total magnetization.

Figure 3 shows the calculated temperature dependence of the longitudinal relaxation time for permalloy doped with 5% Ho. The relaxation time is shown for both sublattices. It can be seen that the rare-earth relaxation time is much longer than that of the transition metal. This, as shown in Fig. 2, is due to the slower increase of the lattice temperature in addition to the intrinsically slower relaxation of the RE due to its large moment. At high temperature, the TM relaxation shows a peak in the relaxation time close to the Curie temperature.

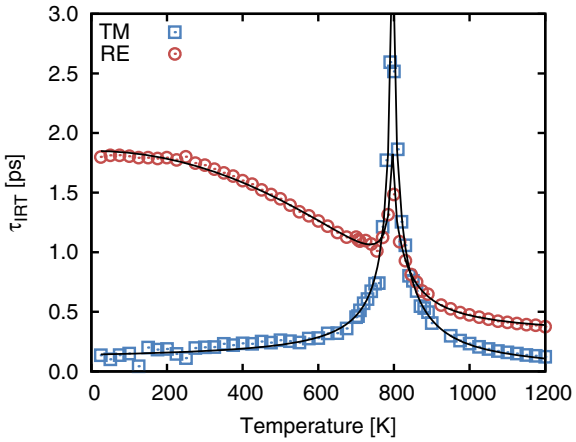

FIG. 3. (Color online) Integral relaxation times for the TM (blue squares) and RE (red circles) sublattices in $Ni_{75}Fe_{20}Ho_5$ for different temperature step sizes. The spins begin in the ground state at 0 K. A Heaviside step function is then applied to the electron temperature changing it to the required value. The TM behaves as expected with a gradual increase until diverging at the Curie temperature. The RE sublattice relaxation time generally decreases but exhibits a peak at the Curie temperature consistent with the coupling to the TM by the interlattice exchange. The solid lines are a guide to the eye showing the divergent behavior.

This is the critical slowing down characteristic of all phase transitions. Interestingly, the RE also exhibits a peak at the T_C, although this temperature is much higher than the RE ordering temperature. This reflects the strong intersublattice exchange with the TM sublattice slowing the relaxation of the RE sublattice.

B. Ferromagnetic resonance simulations

We next investigate the effects of the RE doping on the macroscopic effective Gilbert damping of the system within the atomistic model. As described earlier the effective Gilbert damping is calculated from the motion of the magnetization in an applied field. The calculated results exhibit precession and slow damping back to equilibrium, allowing the determination of the transverse relaxation time and damping parameter by fitting to a damped oscillatory function.

Figure 4 shows the fit to the x component of a selection of concentrations to highlight the effect of doping on the rate of damping in Ho doped permalloy at low temperature. Clearly, the macroscopic damping increases with RE concentration, consistent with experiment. At low doping concentrations the transverse relaxation time is not so short as to seriously limit the number of precession cycles giving an accurate determination of the effective damping parameter α. At higher concentrations, the transverse relaxation time is very short causing the fitting to be less accurate, as shown in Fig. 4(c). Nonetheless, the fit of the damped oscillatory function is still sufficiently good to give a reasonable value of α_{eff}.

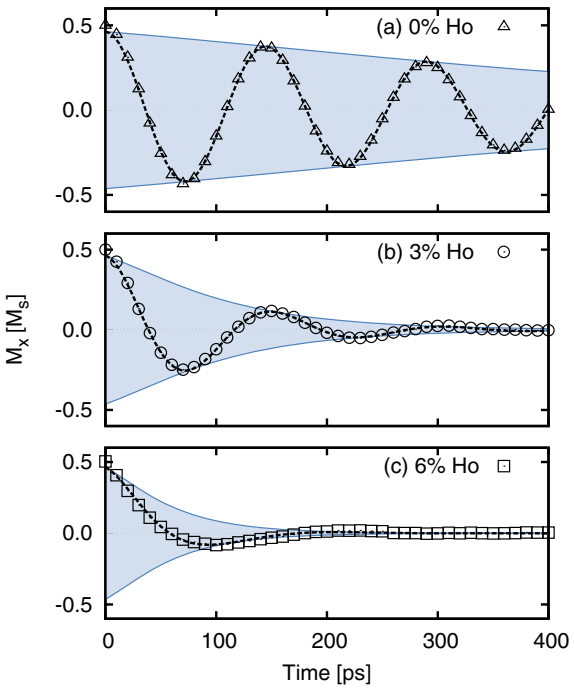

FIG. 4. (Color online) Transverse (x) component of the reduced total magnetization as a function of time after excitation of the system by coherent rotation of the spins to an angle of 30 degrees. Different concentrations are shown highlighting the effect of doping as the concentration is increased from 0% (a) to 6% (c) at 1K. The strength of the applied field was $h = 0.25$ T in all cases, applied along the z axis. The dashed lines represent a fitted $\cos(t/\tau_p)/\cosh(t/\tau_r + d)$ function and the shaded area shows the envelope of the damping function from which the Gilbert damping factor can be extracted. The fitting parameters τ_p and τ_r are the precession and transverse relaxation times, respectively, and for a simple single macrospin, have the values $\tau_p = (1 + \alpha_{\text{eff}}^2)/\gamma h$, $\tau_r = \tau_p/\alpha_{\text{eff}}$. and so the ratio of the times give the damping factor.

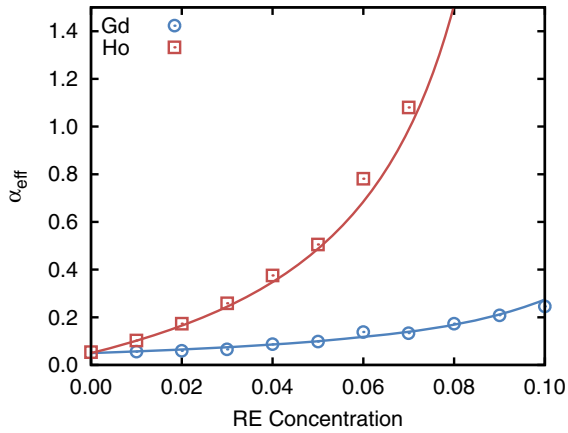

FIG. 5. (Color online) The relation between the RE concentration and the Gilbert damping parameter for Ho (red squares) and Gd (blue circles). The analytic form (lines) for both Ho and Gd from Eq. (17) agrees well with the calculated damping from the model (points) at $T = 1$ K. The damping diverges at the magnetization compensation point where the total M_s is zero as the RE sublattice magnetization completely cancels the TM sublattice magnetization. At low doping concentrations, the change in the damping is almost linear, which agrees well with the results of Ref. 13.

Figure 5 shows the calculated effective Gilbert damping factor as a function of concentration of Gd (blue circles) and Ho (red squares) at 1 K. By modeling the ferrimagnetic system as two coupled sublattices, as in Wangsness *et al.*,[34] an expression for the effective damping of the total magnetization can be derived:

$$\alpha_{\text{eff}} = \frac{M_{\text{TM}}\lambda_e^{\text{TM}} + M_{\text{RE}}\left(\lambda_e^{\text{RE}} + \lambda_l^{\text{RE}}\right)}{M_{\text{TM}} - M_{\text{RE}}}. \qquad (17)$$

As the figure shows the calculations match well with the analytic solution, the damping diverging at the point where the magnetization of the two sublattices cancel.

The model correctly reproduces the effect of RE impurities on damping in permalloy shown experimentally in Refs. 13 and 33. This is an important test of the model and the introduction of an additional damping channel via the strong spin-orbit coupling of the RE spins.

C. Comparison of theory and experiment

Before embarking upon a direct comparison of the model predictions with experiment, we first investigate the theoretical predictions of Refs. 8 and 10 by investigating the longitudinal relaxation time in a system without the complexity of multiple sublattices and energy transfer channels. Specifically, we calculate the IRT as a function of the coupling to the thermal bath for a range of x in $\text{Ni}_x\text{Fe}_{1-x}$. The variation of composition introduces a variation in the effective magnetic moment per atom, μ_{eff}. We neglect any change in the local magnetic moments of Ni and Fe or crystalline structure from the change

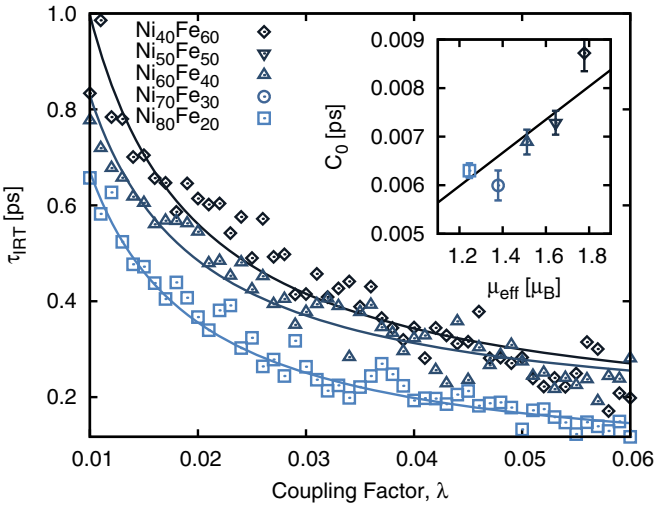

FIG. 6. (Color online) Variation of the longitudinal relaxation time of permalloy (light blue squares), 60% Fe (dark blue triangles), and 40% Fe (black diamonds) as a function of thermal bath coupling calculated using the atomistic model. The solid lines are fitted functions using $\tau_{\mathrm{IRT}} = (C_0/\lambda) + d$. The variation of Fe percentage aims to vary the effective magnetic moment per atom (μ_{eff}) as no structural change is considered. Initially, the system is in an ordered state until a Heaviside step function is applied to $T_e = 300$ K. The relationship matches well with Eqs. (1) and (2). The lines are a fitted function to each data set, for which the constant C_0 is proportional to the magnetic moment as shown in the inset.

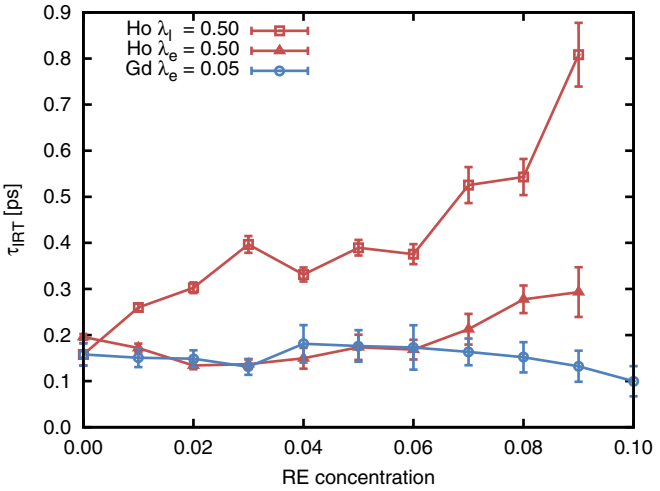

FIG. 7. (Color online) The change in the integral relaxation time of the TM sublattice for a range of concentrations of Ho (red squares and triangles) and Gd (blue circles). Results are shown for Ho coupled to either the lattice (squares) or the electrons (triangles); this shows that the increase of the demagnetization time occurs due to the spin-lattice interaction of Ho. This agrees well with the experimental work of Radu *et al.* apart from a different scale. We find the integral relaxation time is longer than the values of the demagnetization time from the experiments. The behavior is consistent but in disagreement with predictions from Eqs. (1) and (2).

in composition, as this serves to specifically investigate how the change in effective moment changes the longitudinal relaxation.

Figure 6 shows that in this case there is an inverse relation between the demagnetization time and coupling factor, in direct agreement with Ref. 8. The inset shows the fitting parameters for a larger range of compositions and shows that there is linear relation with the effective magnetic moment and fitting parameter, as predicted in Ref. 10. Thus, in this simple case, with all spins coupled to the same heat bath, the analytical model predictions are consistent with the numerical calculations.

We now move to the longitudinal relaxation calculations for the permalloy doped with low concentrations of Ho and Gd. Figure 7 shows the relaxation time as a function of RE concentration for three different cases; Gd is coupled to the electron reservoir (blue circles), Ho coupled to the lattice reservoir (red squares), and Ho coupled to the electrons (red triangles). The first two cases are as discussed previously but the last case is included for comparison. The results clearly show that for higher concentrations of Gd and Ho coupled to the electrons have little effect on the demagnetization time, while when the Ho is coupled to the lattice the demagnetization time increases.

Comparison of our model calculations to the experiments of Radu *et al.*[13] leads to a clear interpretation of the results. Specifically, the coupling of the Ho to the electron reservoir, even with a high damping, does not give the same behavior as observed in the experiments. This supports the assumption that there is a strong interaction between the lattice and the Ho moments. The coupling of the Ho spins to the lattice reservoir shows an increase in the longitundinal relaxation time of approximately a factor of 5 over the range of concentrations between 0% and 10%. This behavior of the relaxation time on the Ho doping and also the behavior with the Gd doping are in agreement with the experimental data, although on a different time scale. This suggests that the energy transfer channel via the lattice heat bath dominates the demagnetization time for the impurity spins in Ho doped permalloy.

In the experiments of Ref. 13, the demagnetization time of the permalloy is found to be about, $\tau_d \sim 75$ fs. In our calculations of the integral relaxation time in Fig. 6, this would correspond to a damping of over 0.1, which for permalloy is too high in relation to the generally accepted experimental value. However, the agreement between theory and experiment in terms of the magnitude of the longitudinal relaxation time to within a factor of 2 is reasonable since the calculation of the electron temperature via the two-temperature model may not give exactly the exact experimental temperature variation. In addition, in Ref. 13, the demagnetization time is fitted to a single exponential where as the integral relaxation time used here accounts for all the eigenmodes of the magnetization relaxation. This along with the model not accounting for the full details of the experiments, such as laser fluence, explain as to why there is a difference in the time scales.

The behavior of the demagnetization time with the RE doping is in disagreement with the prediction of Koopmans' model using the effective damping calculated from the transverse relaxation. Within the atomistic model, the increase arises from the coupling of the Ho spins to the lattice temperature, removing the large damping species from the energy channel associated with the subpicosecond demagnetization, which is by the transfer of energy from the laser into the spin system

via the conduction electrons. Thus the simple model of a single energy transfer channel, cannot be expected to apply, especially when taking the α value from FMR experiments, which involve a different energy transfer channel, specifically the spin/lattice interaction.

Therefore from Figs. 6 and 7 both the theoretical results of Ref. 8 and experimental results of Ref. 13 are exhibited in the Langevin spin model and highlight different effects within it. In the different cases, the energy transfer channels are different; in Fig. 6, the TM is coupled to the electron reservoir, which is found to cause the ultrafast demagnetization. Whilst in the calculations of the doped permalloy, the Ho is coupled to the lattice. For the TM case, the larger the coupling values the stronger the coupling to the electron reservoir causing it to demagnetize faster, which is shown in the results. For the Ho doping case, energy is transferred from the electron reservoir to the lattice reservoir before it causes the demagnetization of the Ho sublattice. So even for the large coupling constants λ_l^{RE} assumed for Ho, the energy transfer via the lattice is a much slower channel leading to the behavior similar to the experimental results presented by Radu *et al.*

IV. CONCLUSION

We have studied the ultrafast demagnetization in RE doped permalloy for comparison with the experiments of Radu *et al.*,[13] which disagree with simple analytical models that predict an inverse dependence on the macroscopic damping parameter. Our computational model reflects two of the possible energy transfer channels responsible for damping. Two coupling factors are used to couple the spins to separate heat baths under the assumption that the laser energy is transferred via an effective increase of the electron temperature into the TM spins with the RE more strongly coupled to the lattice via spin orbit coupling. This model describes the separate dynamics of the transition metal and rare-earth elements, consistent with recent studies.[1,7] This leads to differential dynamic behavior, with the demagnetization time dominated by the interaction between the conduction electrons and TM spins, and the longer timescales associated with FMR dominated by the RE element.

By calculating the longitudinal relaxation time, after a step change in the electron temperature, we can see that at the Curie temperature the TM relaxation time diverges. Due to the exchange coupling between the sublattices the diverging TM relaxation time causes a lengthening in the RE relaxation time. Looking at the case of undoped permalloy, the relaxation time is described well by the theoretical predictions of Koopmans *et al.* with an inverse relationship with the coupling factor.

Ferromagnetic resonance simulations have been carried out in order to calculate the effective macroscopic damping. These simulations have confirmed that the effect of RE impurities is to increase the overall damping of the system with increasing RE concentration, in qualitative agreement with the experimental results of Radu *et al.* Given the increase in macroscopic damping with RE concentration the theoretical models of Refs. 8 and 10 predict a decrease in demagnetization time with RE concentration. Our calculations show a linear increase, consistent with the experimental work of Radu *et al.*[13] This results directly from the coupling of the rare-earth elements to the lattice temperature as expected due to the very strong spin-orbit coupling. Since the relaxation of the rare-earth sublattice is restricted by the thermalization of the lattice temperature it can be seen that this dominates the behavior and the higher concentration of rare-earth impurities reduces the amount of fast relaxing transition metal atoms.

The damping in magnetic materials is a very complex process, that is not controlled by a single mechanism and incorporates a large amount of underlying physics. Here we conclude that in order to describe the ultrafast dynamics of amorphous TM-RE alloys it is necessary to allow two coupling channels. The first couples the TM spins to the conduction electron temperature and the second couples the RE to the lattice. The former is responsible for the ultrafast demagnetization and the latter for the rather slower longitudinal macroscopic relaxation associated with FMR. In complex materials, it is evidently important not to expect a single damping parameter but to consider the energy transfer channel relevant to the technique and time scale of the measurement.

ACKNOWLEDGMENTS

The authors would like to acknowledge financial support of the EU FP7 programme [Grants Nos. NMP3-SL-2008-214469 (UltraMagnetron) and 214810 (FANTOMAS)] and the Nuffield Foundation.

*me521@york.ac.uk

[1] I. Radu *et al.*, Nature (London) **472**, 205 (2011).
[2] C. D. Stanciu, F. Hansteen, A. V. Kimel, A. Kirilyuk, A. Tsukamoto, A. Itoh, and T. Rasing, Phys. Rev. Lett. **99**, 047601 (2007).
[3] J. Hohlfeld, T. Gerrits, M. Bilderbeek, T. Rasing, H. Awano, and N. Ohta, Phys. Rev. B **65**, 012413 (2001).
[4] E. Beaurepaire, J. C. Merle, A. Daunois, and J. Y. Bigot, Phys. Rev. Lett. **76**, 4250 (1996).
[5] J. Hohlfeld, E. Matthias, R. Knorren, and K. Bennemann, Phys. Rev. Lett. **79**, 960 (1997).
[6] A. Scholl, L. Baumgarten, R. Jacquemin, and W. Eberhardt, Phys. Rev. Lett. **79**, 5146 (1997).
[7] T. A. Ostler *et al.*, Nat. Commun. **3**, 666 (2012).
[8] B. Koopmans, J. J. M. Ruigrok, F. DallaLonga, and W. J. M. de Jonge, Phys. Rev. Lett. **95**, 267207 (2005).
[9] T. L. Gilbert, IEEE Trans. Magn. **40**, 3443 (2004).
[10] N. Kazantseva, U. Nowak, R. W. Chantrell, J. Hohlfeld, and A. Rebei, Europhys. Lett. **81**, 27004 (2008).
[11] M. Farle, Rep. Prog. Phys. **61**, 755 (1998).
[12] O. Chubykalo-Fesenko, U. Nowak, R. W. Chantrell, and D. A. Garanin, Phys. Rev. B **74**, 094436 (2006).
[13] I. Radu, G. Woltersdorf, M. Kiessling, A. Melnikov, U. Bovensiepen, J. U. Thiele, and C. H. Back, Phys. Rev. Lett. **102**, 117201 (2009).
[14] S. G. Reidy, L. Cheng, and W. E. Bailey, Appl. Phys. Lett. **82**, 1254 (2003).

[15]M. Fähnle, J. Seib, and C. Illg, Phys. Rev. B **82**, 144405 (2010).
[16]U. Nowak, in *Handbook of Magnetism and Advanced Magnetic Materials*, edited by H. Kronmuller and S. Parkin (Wiley, Hoboken, N.J., 2007), Vol. 2.
[17]A. Lyberatos, D. V. Berkov, and R. W. Chantrell, J. Phys.: Condens. Matter **5**, 8911 (1993).
[18]D. A. Garanin, Phys. Rev. E **54**, 3250 (1996).
[19]S. I. Anisimov, B. L. Kapeliovich, and T. L. Perelman, Zh. Eksp. Teor. Fiz. **66**, 776 (1974) [Sov. Phys. JETP **39**, 375 (1974)].
[20]J. Chen, D. Tzou, and J. Beraun, Int. J. Heat Mass Transf. **49**, 307 (2006).
[21]B. Skubic, J. Hellsvik, L. Nordström, and O. Eriksson, J. Phys.: Condens. Matter **20**, 315203 (2008).
[22]T. A. Ostler, R. F. L. Evans, R. W. Chantrell, U. Atxitia, O. Chubykalo-Fesenko, I. Radu, R. Abrudan, F. Radu, A. Tsukamoto, A. Itoh, A. Kirilyuk, T. Rasing, and A. Kimel, Phys. Rev. B **84**, 024407 (2011).
[23]L. D. Landau and E. M. Lifshitz, Phys. Z. Sowjetunion **8**, 135 (1935).
[24]Z. Lin and L. V. Zhigilei, Appl. Surf. Sci. **253**, 6295 (2007).
[25]A. Rebei and J. Hohlfeld, Phys. Rev. Lett. **97**, 117601 (2006).
[26]M. Wietstruk, A. Melnikov, C. Stamm, T. Kachel, N. Pontius, M. Sultan, C. Gahl, M. Weinelt, H. A. Dürr, and U. Bovensiepen, Phys. Rev. Lett. **106**, 127401 (2011).
[27]J. Seib and M. Fähnle, Phys. Rev. B **82**, 064401 (2010).
[28]J. H. Mentink, M. V. Tretyakov, A. Fasolino, M. I. Katsnelson, and T. Rasing, J. Phys.: Condens. Matter **22**, 176001 (2010).
[29]M. D'Aquino, C. Serpico, and G. Miano, J. Comput. Phys. **209**, 730 (2005).
[30]D. Lewis and N. Nigam, J. Comput. Appl. Math. **151**, 141 (2003).
[31]O. Bottauscio and A. Manzin, IEEE Trans. Magn. **47**, 1154 (2011).
[32]I. Radu (private communication).
[33]G. Woltersdorf, M. Kiessling, G. Meyer, J. U. Thiele, and C. H. Back, Phys. Rev. Lett. **102**, 257602 (2009).
[34]R. K. Wangsness, Phys. Rev. **91**, 1085 (1953).